Mats Isaksson
Electrical and Computer Engineering Department,
Colorado State University,
Fort Collins, CO 80523
e-mail: mats.isaksson@gmail.com

Kristan Marlow
Institute for Intelligent Systems
Research and Innovation,
Deakin University,
Waurn Ponds Campus,
Geelong, VIC 3217, Australia
e-mail: kristan.marlow@gmail.com

Anthony Maciejewski
Electrical and Computer Engineering Department,
Colorado State University,
Fort Collins, CO 80523
e-mail: aam@engr.colostate.edu

Anders Eriksson
School of Electrical Engineering and
Computer Science,
Queensland University of Technology,
GPO Box 2434,
Brisbane, QLD 4001 Australia
e-mail: anders.eriksson@qut.edu.au

Novel Fault-Tolerance Indices for Redundantly Actuated Parallel Robots

Robots designed for space applications, deep sea applications, handling of hazardous material and surgery should ideally be able to handle as many potential faults as possible. This paper provides novel indices for fault tolerance analysis of redundantly actuated parallel robots. Such robots have the potential for higher accuracy, improved stiffness, and higher acceleration compared to similar-sized serial robots. The faults considered are free-swinging joint failures (FSJFs), defined as a software or hardware fault, preventing the administration of actuator torque on a joint. However, for a large range of robots, the proposed indices are applicable also to faults corresponding to the disappearance of a kinematic chain, for example, a breakage. Most existing fault tolerance indices provide a ratio between a robot's performance after the fault and the performance before the fault. In contrast, the indices proposed in this paper provide absolute measures of a robot's performance under the worst-case faults. The proposed indices are based on two recently introduced metrics for motion/force transmission analysis of parallel robots. Their main advantage is their applicability to parallel robots with arbitrary degrees-of–freedom (DOF), along with their intuitive geometric interpretation. The feasibility of the proposed indices is demonstrated through application on a redundantly actuated planar parallel mechanism. [DOI: 10.1115/1.4035587]

1 Introduction

For certain robot applications, including space robotics, deep sea robotics, and handling of hazardous material, replacing or mending a malfunctioning robot is typically difficult, time consuming, and dangerous. For other robot applications, such as surgery, it is essential that the robot is able to finish a task or perform a controlled retraction after a malfunction. Merely halting the robot is typically not acceptable. Hence, fault-tolerant robots, designed in order to handle as many potential failures as possible, are of significant practical interest.

Maciejewski [1] introduced the concept of robot fault tolerance and showed how a serial kinematically redundant mechanism can be fault tolerant for locked joint failures (LJFs). A LJF means that a joint is assumed to be locked after a failure has occurred. For a kinematically redundant mechanism, the degrees-of-freedom (DOFs) is larger than the DOFs of its end effector. The second main type of redundancy is redundantly actuated mechanism, for which the number of actuators is larger than the DOFs. Note that these definitions permit a mechanism to be both kinematically redundant and redundantly actuated. Such a mechanism has the characteristics of both a redundantly actuated mechanism (potential to introduce stress in the mechanism by operating the actuators independently) and a kinematically redundant mechanism (infinitely many solutions to the inverse kinematics).

Fault tolerance for serial robots has subsequently received considerable academic attention [2–4]. The majority of papers on robot fault tolerance have focused on LJFs. A free-swinging joint failure (FSJF) is a different type of joint failure, corresponding to an actuated joint becoming a passive joint. Such faults are also referred to as torque failures [5]. In Ref. [6], FSJFs for serial robots were handled by utilizing gravity to achieve partial control of the passive joint. It was shown that the fault-tolerant workspace could be increased by utilizing active braking to let the joint vary between locked and free swinging. However, for most practical applications, it would typically be preferable to transform the FSJF to an LJF by applying a brake. The idea of employing two or more serial robots to cooperatively manipulate an object has been investigated in Refs. [7,8]. One advantage of such arrangements is their potential to handle FSJFs [8].

This paper is focused on the fault tolerance of parallel robots. Parallel robots have the potential for higher accuracy, improved stiffness, and higher acceleration compared to similar-sized serial robots.

For a nonredundant parallel mechanism, an LJF would typically lead to a large reduction of the mechanism's workspace and mobility. The reason is that the chain including the locked joint would normally impose a significant constraint on the possible motion. Consider for example a planar 2-RRR mechanism including six revolute joints with parallel joint axes. Each of the two identical chains includes one actuated revolute joint and two passive revolute joints, where the last joint in the two chains is coaxial. Before a fault, the common axis of the last revolute joint in the chains may be positioned in a plane perpendicular to the joint axes. After an LJF, the only possible motion of this axis is a circle in the same plane. Introducing additional actuated chains does not provide tolerance of LJFs in a worst-case scenario, as the actuated joints of the original chains may still be locked at a fault, leading to the same issues as before. A different approach is to include additional actuators in the existing chains. If this is done by actuating a previously passive joint, it leads to a redundantly actuated mechanism, for which the previously discussed issues remain. However, if instead a new actuated joint is introduced, it leads to a kinematically redundant mechanism, with better potential to handle LJFs. If the new actuated joint is positioned very close to an existing joint and is of the same type as this joint, such a mechanism has the potential to maintain similar performance after an LJF. However, in order to be able to handle a worst-case scenario with an arbitrary actuated joint suffering an LJF, the number of actuated joints would have to be doubled compared to a nonredundant mechanism.

Contributed by the Mechanisms and Robotics Committee of ASME for publication in the JOURNAL OF MECHANICAL DESIGN. Manuscript received July 13, 2016; final manuscript received December 15, 2016; published online January 31, 2017. Assoc. Editor: Oscar Altuzarra.

As stated in the previous paragraph, in order for a parallel mechanism to handle LJFs in a worst-case scenario, a large number of actuators are required. In this paper, we instead focus on FSJFs. An LJF could potentially be turned into an FSJF by disengaging the faulty actuator. If a mechanism is not redundantly actuated, an FSJF would lead to an unconstrained DOF when all actuators are locked. As this is typically not acceptable, we only consider redundantly actuated mechanisms. There are two main types of actuation redundancy [9]. A redundantly actuated mechanism may be created from a nonredundant parallel mechanism by actuating a previously passive joint or by introducing an additional actuated chain without modifying the mobility of the mechanism. A combination of these approaches is also possible. In general, utilizing only one actuator per kinematic chain is preferable as such mechanisms have the potential for mounting all actuators on the fixed base, thereby reducing the moving mass of the mechanisms. Hence, the analysis in this paper is focused on redundantly actuated parallel mechanisms including one actuator per kinematic chain.

Indices used to quantify the fault tolerance for FSJFs within these mechanisms will be introduced. For a large range of mechanisms, the same indices are applicable also to failures corresponding to a kinematic chain disappearing. Such failures were named link failures (LFs) by Notash and Huang [10] and referred to as hard failures by Yi et al. [11]. Both an FSJF and an LJF could be turned into an LF by removing the malfunctioning chain. Several other failure types, such as sensor failures, are listed in Ref. [10]; however, they will not be considered here.

Yi et al. [11] introduced local fault tolerance measures to analyze LJFs, FSJFs, and LFs. The proposed measures were based on the percent of manipulability retained after failure; hence, they provide a measure on how much the present performance is reduced due to a specified fault. In contrast, the indices proposed in this paper provide an absolute worst-case measure of the mechanism's performance in each configuration in case of a fault. The proposed indices are based on the motion/force transmission analysis of each kinematic chain within a parallel mechanism. They are independent of the scale of a mechanism and have the advantage of being applicable to mechanisms with both rotational and translational DOFs. The latter is a major advantage compared to indices based on the Jacobian.

The remainder of this paper is organized as follows: Section 2 provides a brief introduction to screw theory and screw theory-based singularity performance indices. In particular, it reviews the input transmission index (ITI), the output transmission index (OTI), and the local minimized transmission index (LMTI). Section 3 introduces the proposed fault tolerance indices, which are extensions of the reviewed indices. In Sec. 4, the proposed fault tolerance indices are applied to a 3-DOF planar parallel mechanism. Finally, Sec. 5 provides conclusion along with directions for future work.

2 Singularity Performance Indices Based on Screw Theory

A unit screw is a six-dimensional vector defined as $\hat{\$} = [\hat{\mathbf{s}}^{\mathrm{T}} \mathbf{s}_{\mathrm{O}}^{\mathrm{T}}]^{\mathrm{T}}$, where $\hat{\mathbf{s}}$ is a three-dimensional unit vector along the screw axis and $\mathbf{s}_{\mathrm{O}}$ is a three-dimensional vector defined by $\mathbf{s}_{\mathrm{O}} = h\hat{\mathbf{s}} + \mathbf{r}_{\mathrm{O}} \times \hat{\mathbf{s}}$. The variable h represents the pitch of the screw and $\mathbf{r}_{\mathrm{O}}$ is a position vector to any point on the screw's axis in an arbitrarily selected coordinate system. Screws can be used to represent both the instantaneous motion of a rigid body, that is, its twist, and the system of forces and moments acting on a rigid body, that is, a wrench. A wrench is described by the product of the wrench's intensity and a unit screw, while a twist is described by the product of the twist's amplitude and a unit screw. The amplitude and intensity are not required for the indices discussed herein; therefore, unit screws are utilized to represent both twists and wrenches. There are two important special cases for the screw pitch h, the first when $h = 0$ and the second when $h = \infty$. The physical interpretations of wrenches and twists with these values of the pitch are described in Table 1.

Table 1 Twists and wrenches with zero pitch and infinite pitch [12]

	$h = 0$	$h = \infty$
Twist	Rotation about $\hat{\mathbf{s}}$ at $\mathbf{r}_{\mathrm{O}}$	Translation along $\hat{\mathbf{s}}$ (free vector)
Wrench	Force along $\hat{\mathbf{s}}$ at $\mathbf{r}_{\mathrm{O}}$	Moment about $\hat{\mathbf{s}}$ (free vector)
Unit screw	$\begin{bmatrix} \hat{\mathbf{s}} \\ \mathbf{r}_{\mathrm{O}} \times \hat{\mathbf{s}} \end{bmatrix}$	$\begin{bmatrix} \mathbf{0}_{(3\times1)} \\ \hat{\mathbf{s}} \end{bmatrix}$

The reciprocal product plays an important role in the theory of screws. Given a twist and a wrench, the absolute value of their reciprocal product is the instantaneous work performed by the wrench on the twist. A zero value of this product signifies that the screws are reciprocal, that is, the wrench does not perform any work on the twist. The reciprocal product forms the foundation of the motion/force transmission analysis. It is defined as

$$\hat{\$}_1 \circ \hat{\$}_2 = \hat{\mathbf{s}}_1 \cdot \mathbf{s}_{\mathrm{O}_2} + \mathbf{s}_{\mathrm{O}_1} \cdot \hat{\mathbf{s}}_2 \tag{1}$$

where $\circ$ is the reciprocal product operator. If both screws have infinite pitch, the reciprocal product equals zero, while if neither of the screws has infinite pitch, the reciprocal product can be written as

$$\hat{\$}_1 \circ \hat{\$}_2 = (h_1 + h_2)\cos\upsilon - \rho \sin\upsilon \tag{2}$$

where h_1 and h_2 are the pitch of each screw, ρ is the length of the common perpendicular between the screw axes, and υ is the angle between the screws' axes. The expression $(1/2)((h_1 + h_2)\cos\upsilon - \rho \sin\upsilon)$ was referred to as the virtual coefficient by Ball [13]. If the two screw axes are perpendicular, Eq. (2) can be simplified to

$$\hat{\$}_1 \circ \hat{\$}_2 = -\rho \tag{3}$$

The performance of a parallel mechanism is affected both in an exact singular configuration and in its vicinity. Hence, indices for evaluating the distance to singularities are of utmost importance. Sutherland and Roth [14] proposed to employ the normalized reciprocal product as a transmission index for a single-loop linkage. This work formed the foundation of the transmissivity proposed by Tsai and Lee [15], the generalized transmission index presented by Chen and Angeles [16], and the power coefficient introduced by Wang et al. [17]. The main difference between the proposed indices is the definition of the normalization factor. Sutherland and Roth's index is not applicable if the screws are parallel or one of their pitches is infinite, while Tsai and Lees' index is not frame invariant. Chen and Angeles generalized the index calculation to also include cases with parallel screw axes and infinite pitch of one of the screws. Their method provides the result by Sutherland and Roth as a special case. Furthermore, Chen and Angeles utilized a constant global maximum of the normalization factor, in order to more closely relate to the distribution of the unnormalized reciprocal product. However, for some mechanisms, as those investigated herein, the normalization factors become close to infinity in certain configurations, leading to index values approaching zero in most other configurations. In contrast, Wang et al. [17] made use of the local maximum of the normalization factor, resulting in a clear relation between the motion/force transmission ability of a wrench on its associated twist. However, a drawback of this approach is that configurations where both the reciprocal product and the normalization factor are close to zero may still provide an optimal unity value of the index. In such configurations, the index is a poor measure of a mechanism's performance. For the proposed indices, we will utilize the local maximum of the normalization factor. Therefore, an analysis

of the effects of the described issue on the proposed indices has been included.

The power coefficient, proposed by Wang et al. [17], is defined according to

$$\mathrm{PC} = \frac{\left|\hat{\$}_1 \circ \hat{\$}_2\right|}{\left|\hat{\$}_1 \circ \hat{\$}_2\right|_{\max}} \tag{4}$$

where the numerator represents the magnitude of the reciprocal product between a unit wrench $\hat{\$}_1$ and a unit twist $\hat{\$}_2$, and the denominator is its potential maximum magnitude. The denominator is calculated according to

$$|\hat{\$}_1 \circ \hat{\$}_2|_{\max} = \sqrt{(h_1 + h_2)^2 + \rho_{\max}^2} \tag{5}$$

where h_1 and h_2 are the pitches of the two screws and $\rho_{\max}$ is the potential maximum length of the common perpendicular between the wrench and the twist, calculated by rotating the actuation wrench at a characteristic point on the wrench, typically coinciding with one joint position. The power coefficient relates only to the parameters of the two screws. It provides frame invariant results with a range from zero to unity. For the special case of $\hat{\$}_1 \circ \hat{\$}_2 = 0$, the expression (4) equals zero by definition. This case occurs if $\hat{\$}_1$ and $\hat{\$}_2$ are intersecting zero pitch screws.

Wang et al. [17] utilized the power coefficient to define two indices, termed the input transmission index (ITI) and the output transmission index (OTI), defining the input and output performance of a parallel mechanism, respectively. Additionally, it was proposed to use the minimum of these values as a local transmission index (LTI). These indices have been applied to nonredundant, purely parallel mechanisms in Refs. [12,18–21]. The OTI and ITI form the basis for the fault tolerance analysis in this paper. They are dimensionless, frame invariant, and can be applied to purely rotational, purely translational, and combined motion parallel mechanisms.

The ITI for a kinematic chain i indicates the normalized instantaneous work performed between the chain's actuation wrench $\hat{\$}_{\mathrm{A},i}$ and its input twist $\hat{\$}_{\mathrm{I},i}$

$$\mathrm{ITI}_i = \frac{|\hat{\$}_{\mathrm{A},i} \circ \hat{\$}_{\mathrm{I},i}|}{|\hat{\$}_{\mathrm{A},i} \circ \hat{\$}_{\mathrm{I},i}|_{\max}} \tag{6}$$

The input twist $\hat{\$}_{\mathrm{I},i}$ is the twist of the actuated joint of chain i. The generalized forces that can be transmitted from the tool platform to the fixed base with a chain's actuated joints unlocked are referred to as the constraint wrenches of a chain. The actuation wrench $\hat{\$}_{\mathrm{A},i}$ of a chain is the generalized forces, in addition to the constraint wrenches, that can be can be transmitted with the actuated joints of the chain locked. The actuation wrench is also referred to as the transmission wrench screw [16]. It is reciprocal to the twists of all passive joints in its respective chain.

The overall ITI for a nonredundant mechanism with n such chains is calculated as

$$\mathrm{ITI} = \min(\mathrm{ITI}_i), \quad i = 1 \ldots n \tag{7}$$

An ITI value of zero is equivalent to a type one singularity [22] of the mechanism.

The OTI for a kinematic chain i is the normalized instantaneous work performed between $\hat{\$}_{\mathrm{A},i}$ and its output twist $\hat{\$}_{\mathrm{O},i}$

$$\mathrm{OTI}_i = \frac{|\hat{\$}_{\mathrm{A},i} \circ \hat{\$}_{\mathrm{O},i}|}{|\hat{\$}_{\mathrm{A},i} \circ \hat{\$}_{\mathrm{O},i}|_{\max}} \tag{8}$$

where the output twist is defined as the platform's free motion when all actuators, except the actuator of the chain under examination, are locked. The overall OTI for a nonredundant mechanism with n chains is calculated according to

$$\mathrm{OTI} = \min(\mathrm{OTI}_i), \quad i = 1 \ldots n \tag{9}$$

The OTI analyzes the interactions between the chains of a mechanism. A zero value is equivalent to a type two singularity [22].

In order to limit the scope of this paper, mechanisms subjected to constraint singularities [23] are not considered herein. However, the proposed fault tolerance analysis may be extended to such mechanisms by also considering the constraint transmission index proposed by Liu et al. [24] and the intrachain constraint index proposed by Marlow et al. [21].

3 Fault Tolerance Indices for Redundantly Actuated Parallel Mechanisms

As motivated in the introduction, herein we only consider FSJFs of redundantly actuated parallel mechanisms including more kinematic chains than DOFs. For all such mechanisms, the actuators that cannot be moved freely when all other actuators are locked are termed mutual interference actuators [25]. These actuators are either all the actuators in a mechanism or a subset of these actuators. A redundantly actuated mechanism will generate internal forces within the link system if the mutual interference actuators are operated independently. In order to avoid wear and potential breakage of the mechanism, such mechanisms should be controlled using advanced control algorithms, where the coordination of the actuators plays a central role [26]. However, redundantly actuated mechanisms feature several advantages, including the possibility to eliminate singularities [27] and the possibility to optimize the contact forces that can be generated or withstood by the mechanisms end-effector [28].

While a redundantly actuated parallel mechanism typically[1] has limited solutions to the inverse kinematics problem, it has infinite solutions to the inverse dynamics problem, i.e., there are infinitely many combinations of actuator torques leading to the same tool wrench. Nokleby et al. [28] proposed methods to select the actuator torques that maximize the tool wrench. For a redundantly actuated mechanism, it is not possible to evaluate the motion/force transmissibility exactly [25]. However, it is possible to use the local minimized transmission index (LMTI) proposed by Xie et al. [25] as a lower bound on the OTI of a redundantly actuated mechanism.

In case an actuator is not a mutual interference actuator, modifying the actuated joint to a passive joint means the manipulated platform is not constrained when all remaining actuated joints are locked. Consider for example the 4-RPR mechanism in Fig. 1. The actuators of chains 1–3 are mutual interference actuators while the actuator of chain 4 is not. If the actuated joint of chain 4 is modified to a passive joint, the platform is no longer fully constrained when all remaining actuated joints are locked. The fault tolerance indices proposed in this paper are worst-case measures and return a zero value if the platform cannot be fully constrained after a fault. The following derivation is made more readable by assuming all actuators are mutual interference actuators; however, the derived indices provide a correct value (zero) also if this is not the case.

Consider an n-DOF redundantly actuated mechanism with a mutual interference actuators given by the set $\mathbf{A}$. We denote the LMTI of such a mechanism by ${}^{a}\mathrm{LMTI}_{\mathbf{A}}$. By selecting n actuators from the set $\mathbf{A}$, it is possible to create $\binom{a}{n}$ unique nonredundant submechanisms, each including the n actuators specified by the set

$$\mathbf{N}_i = i\text{:th } n\text{-combination of } \mathbf{A}, \quad i = 1 \ldots \binom{a}{n} \tag{10}$$

[1]The exception is a mechanism that is both redundantly actuated and kinematically redundant.

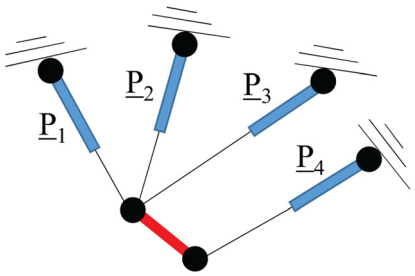

Fig. 1 A 3-DOF planar redundantly actuated 4-RPR mechanism

The OTI for each of these submechanisms is denoted by $\mathrm{OTI}_{\mathbf{N}_i}$ and calculated according to Eqs. (8) and (9). Thereafter, ${}^{a}\mathrm{LMTI}_{\mathbf{A}}$ is calculated according to

$$ {}^{a}\mathrm{LMTI}_{\mathbf{A}} = \max(\mathrm{OTI}_{\mathbf{N}_i}), \quad i = 1\ldots\binom{a}{n} \tag{11} $$

The LMTI value is zero for mechanisms that are not fully constrained when all actuators are locked, as all corresponding OTI values are zero.

We will extend the use of the ITI in Eq. (7) to a redundantly actuated mechanism. This index is appropriate as long as the actuators of all chains are permanently engaged. Due to limitations in actuator speed, a poor performance of one chain close to the workspace edge cannot be compensated for by the other chains. However, if a mechanism has a possibility to disengage the actuators of the worst performing chain, this index is not suitable.

We now proceed to propose several indices that quantify the fault tolerance for FSJFs of redundantly actuated mechanisms, meaning faults when an actuated joint is changed to a passive joint. The proposed fault tolerance indices are based on the OTI, ITI, and LMTI discussed previously and provide a measure between zero and one, indicating the performance of a mechanism after a worst-case fault has occurred. Each index is absolute, meaning the indices can be utilized to compare different architectures, as well as the relative performance of a mechanism in different configurations. For a redundantly actuated mechanism with a mutual interference actuators and n DOFs ($a > n$), we introduce $(a-n)$ output fault tolerance indices $\mathrm{F}_{\mathrm{O}j}$ and $(a-n)$ input–output fault tolerance indices $\mathrm{F}_{\mathrm{IO}j}$, where $j = 1\ldots(a-n)$ is the number of actuated joints that potentially suffer an FSJF. The index values for each j are in general different, meaning the optimal configuration for a mechanism to suffer one arbitrary FSJF is not the same as the optimal configuration to suffer two arbitrary FSJF, etc. The indices $\mathrm{F}_{\mathrm{O}j}$ are defined as

$$ \mathrm{F}_{\mathrm{O}j} = \begin{cases} \min(\mathrm{OTI}_{\mathbf{E}_i}), i = 1\ldots\binom{a}{n} & \text{if } j = a-n \\ \min({}^{a-j}\mathrm{LMTI}_{\mathbf{E}_i}), i = 1\ldots\binom{a}{a-j} & \text{if } j < a-n \end{cases} \tag{12} $$

where the sets $\mathbf{E}_i$ are given by

$$ \mathbf{E}_i = i\text{:th } (a-j)\text{-combination of } \mathbf{A} \tag{13} $$

and the expressions ${}^{a-j}\mathrm{LMTI}_{\mathbf{E}_i}$ are calculated according to Eq. (11). As discussed previously, if not all actuators are mutual interference actuators, the indices $\mathrm{F}_{\mathrm{O}j}$ (12) will all be zero.

The input–output fault tolerance indices $\mathrm{F}_{\mathrm{IO}i}$ are calculated by taking the minimum of $\mathrm{F}_{\mathrm{O}i}$ and the ITI of the redundantly actuated mechanism according to

$$ \mathrm{F}_{\mathrm{IO}j} = \min(\mathrm{F}_{\mathrm{O}j}, \mathrm{ITI}) \tag{14} $$

where the ITI is determined from Eq. (7). According to the previous discussion, the ITI index, and hence the $\mathrm{F}_{\mathrm{IO}j}$ index, is only suitable for mechanisms where all actuators are permanently engaged.

If each kinematic chain only includes one actuator and if the chain either does not provide a constraint wrench (e.g., an RSS chain or a UPS chain) or if the provided constraint wrench is duplicated by other linkages (as in multiple RRR chains), the fault tolerance indices are valid also for the case of an LF.

The fault tolerance indices $\mathrm{F}_{\mathrm{O}j}$ and $\mathrm{F}_{\mathrm{IO}j}$ describe the worst-case performance for j FSJFs. It may also be useful to introduce indices for other than the worst cases. For example, by modifying Eq. (12) to calculate an average of the OTI and LMTI values instead of a minimum. However, we will not further consider this possibility.

4 Example

In this section, we apply the proposed fault tolerance indices to a 3-DOF planar parallel mechanism with two translational DOFs and one rotational DOF. The investigated mechanism is illustrated in Fig. 2. It includes a fixed base and a manipulated platform, connected by five identical kinematic chains. As demonstrated in Fig. 2(*b*), the manipulated platform can be designed in order to avoid any collisions between the platform and the lower arm links, while potential collisions between the upper arm links and the platform joint axis of the same chain are avoided by limiting the smallest allowed elbow angle between the upper arm link and the lower arm link in the same chain.

A fixed coordinate system $\mathbf{F}$ is defined according to Fig. 2(*a*). Each kinematic RRR chain i is composed of an actuated revolute joint with joint axis at $\mathbf{b}_i = [b_{ix}\, b_{iy}]^{\mathrm{T}}$, an upper arm link of length a_i, a passive revolute joint with joint axis at $\mathbf{c}_i = [c_{ix}\, c_{iy}]^{\mathrm{T}}$, a lower arm link of length l_i, and passive revolute joint with joint axis at $\mathbf{d}_i = [d_{ix}\, d_{iy}]^{\mathrm{T}}$ on the manipulated platform. In order to improve the readability of Fig. 2(*a*), the positions $\mathbf{d}_i$ are not marked; however, they are identified as the platform joint connected to link l_i.

A second coordinate system $\mathbf{M}$ is defined fixed relative to the manipulated platform. The origin of $\mathbf{M}$ is in the center of the five platform joints $\mathbf{d}_i$. Its x-axis intersects the joint position $\mathbf{d}_1$, while its y-axis is determined according to the right-hand rule assuming the z-axis is directed out of the paper. The origin of $\mathbf{M}$ in $\mathbf{F}$ is given by $\mathbf{r}$, while its orientation is given by the rotation matrix $\mathbf{R}(\phi)$, where

$$ \mathbf{r} = [x\, y]^{\mathrm{T}} \tag{15} $$

$$ \mathbf{R}(\phi) = \begin{bmatrix} \cos\phi & -\sin\phi \\ \sin\phi & \cos\phi \end{bmatrix} \tag{16} $$

The locations of the platform joints are specified in $\mathbf{M}$ by ${}^{\mathbf{M}}\mathbf{d}_i$. These locations can be transformed to the fixed coordinate system $\mathbf{F}$ according to $\mathbf{d}_i = \mathbf{r} + \mathbf{R}(\phi){}^{\mathbf{M}}\mathbf{d}_i$.

All actuators are mutual interference actuators according to the definition in Section 3. Each of the RRR chains provides two identical constraints on the platform orientation and one identical constraint on the position in the z-direction. For mechanisms of this type, the fault tolerance indices can be applied to both FSJFs and LFs.

By employing more than three RRR chains, it is possible to design a mechanism with the capability of infinite platform rotation in large areas of the workspace. In this paper, we analyze the fault tolerance of a mechanism with five RRR chains. As infinite tool rotation requires at least four kinematic chains, we only study the case of a single FSJF or a single LF.

Designing an optimally fault tolerant mechanism of this type is not straightforward and not attempted in this paper. We will here

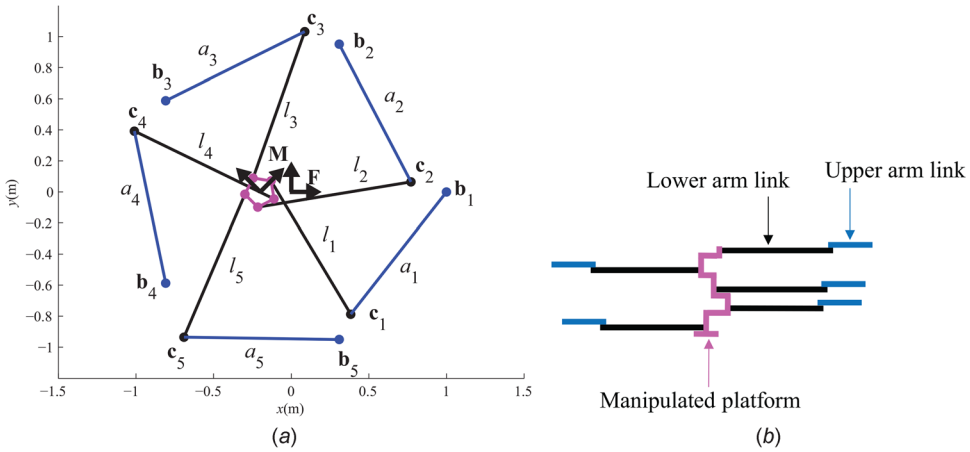

Fig. 2 A redundantly actuated 3-DOF planar parallel mechanism with five actuators. (*a*) Top view of the mechanism and (*b*) side view, demonstrating how the mechanism can be designed in order to avoid collisions between the lower arm links and the manipulated platform when it is rotated.

merely demonstrate the fault tolerance of one potential mechanism variant. The studied variant was selected by arranging both the base joints and the platform joints in two regular pentagons and using identical lengths for all upper and lower arm links. There are $5! = 120$ possible permutations on how to connect the five base joints to the platform joints. The selected arrangement, shown in Fig. 2(*a*), was found by evaluating all 120 design permutations during a full platform rotation in the center of the workspace. The variant exhibiting the largest minimum value of the output fault tolerance index F_{O1} during this rotation was selected. Its parameter values are summarized in Table 2.

The joint locations $\mathbf{c}_i$ are given by the intersection of two circles, one with an origin at $\mathbf{b}_i$ and radius a_i and another with origin at $\mathbf{d}_i$ and radius l_i. The utilized working mode of each chain is as illustrated in Fig. 2(*a*). The inverse kinematics calculations for this mechanism are straightforward and will not be detailed here.

We begin by calculating the OTI and the ITI for a nonredundant submechanism of the studied mechanism. Such a submechanism is obtained by removing two of the kinematic chains from the mechanism in Fig. 2(*a*) and has the remaining kinematic chains k, l, and m. The ITI for this submechanism is calculated according to

$$\mathrm{ITI}_{klm} = \min(\mathrm{ITI}_k, \mathrm{ITI}_l, \mathrm{ITI}_m) = \min\left(\frac{|\hat{\$}_{\mathrm{A},i} \circ \hat{\$}_{\mathrm{I},i}|}{|\hat{\$}_{\mathrm{A},i} \circ \hat{\$}_{\mathrm{I},i}|_{\max}}\right), \quad i = k,l,m \tag{17}$$

where $\hat{\$}_{\mathrm{A},i}$ is the actuation wrench of chain i and $\hat{\$}_{\mathrm{I},i}$ is the input twist of chain i. As illustrated in Fig. 3(*a*), the actuation wrench is a zero pitch screw directed along the axis of the passive linkage [12], while the input twist is a zero pitch screw directed along the axis of the actuated joint. The calculations are equivalent for each kinematic chain i. We introduce the normalized vectors $\mathbf{f}_i$, $\mathbf{g}_i$, and $\mathbf{f}_{3i}$ according to

Table 2 Kinematic parameters for the mechanism in Fig. 2, $i = 1 \ldots 5$

$a_i = 1.0\,\mathrm{m}$	$\mathbf{b}_i = e[\ \cos((i-1)\gamma) \quad \sin((i-1)\gamma)\ ]^{\mathrm{T}}$
$l_i = 1.0\,\mathrm{m}$	${}^{\mathrm{M}}\mathbf{d}_1 = g[\ 1 \quad 0\ ]^{\mathrm{T}}$
$e = 1.0\,\mathrm{m}$	${}^{\mathrm{M}}\mathbf{d}_2 = g[\ \cos(3\gamma) \quad \sin(3\gamma)\ ]^{\mathrm{T}}$
$g = 0.1\,\mathrm{m}$	${}^{\mathrm{M}}\mathbf{d}_3 = g[\ \cos(\gamma) \quad \sin(\gamma)\ ]^{\mathrm{T}}$
$\gamma = \frac{2\pi}{5}$	${}^{\mathrm{M}}\mathbf{d}_4 = g[\ \cos(4\gamma) \quad \sin(4\gamma)\ ]^{\mathrm{T}}$
	${}^{\mathrm{M}}\mathbf{d}_5 = g[\ \cos(2\gamma) \quad \sin(2\gamma)\ ]^{\mathrm{T}}$

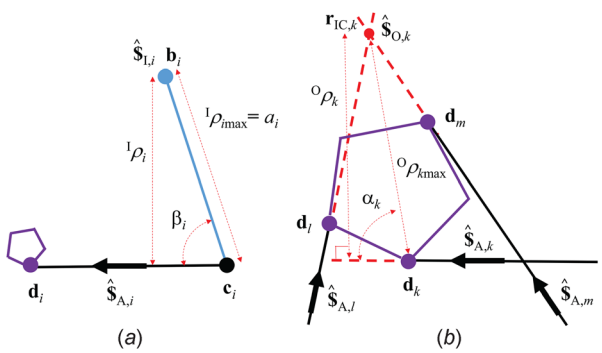

Fig. 3 Calculation of ITI (*a*) and OTI (*b*) for one chain of a nonredundant submechanism obtained by removing two kinematic chains from the mechanism in Fig. 2(*a*). (*a*) ${}^{\mathrm{I}}\rho_i$ is the length of the common perpendicular between the screws $\hat{\$}_{\mathrm{A},i}$ and $\hat{\$}_{\mathrm{I},i}$ while ${}^{\mathrm{I}}\rho_{i\mathrm{max}}$ is the maximum length of the common perpendicular obtained by rotating $\hat{\$}_{\mathrm{A},i}$ around $\mathbf{c}_i$ and (*b*) ${}^{\mathrm{O}}\rho_k$ is the length of the common perpendicular between the screws $\hat{\$}_{\mathrm{A},k}$ and $\hat{\$}_{\mathrm{O},k}$ while ${}^{\mathrm{O}}\rho_{k\mathrm{max}}$ is the maximum length of the common perpendicular obtained by rotating $\hat{\$}_{\mathrm{A},k}$ around $\mathbf{d}_k$.

$$\mathbf{f}_i = \frac{\mathbf{d}_i - \mathbf{c}_i}{l_i} \tag{18}$$

$$\mathbf{g}_i = \frac{\mathbf{c}_i - \mathbf{b}_i}{a_i} \tag{19}$$

$$\mathbf{f}_{3i} = \begin{bmatrix} \mathbf{f}_i \\ 0 \end{bmatrix} \tag{20}$$

The actuation wrench $\hat{\$}_{\mathrm{A},i}$ and the input twist $\hat{\$}_{\mathrm{I},i}$ can be expressed according to

$$\hat{\$}_{\mathrm{A},i} = \begin{bmatrix} \mathbf{f}_{3i} \\ \mathbf{d}_{3i} \times \mathbf{f}_{3i} \end{bmatrix} \tag{21}$$

$$\hat{\$}_{\mathrm{I},i} = \begin{bmatrix} \hat{\mathbf{z}} \\ \mathbf{b}_{3i} \times \hat{\mathbf{z}} \end{bmatrix} \tag{22}$$

where $\mathbf{d}_{3i} = [\mathbf{d}_i^{\mathrm{T}}\ 0]^{\mathrm{T}}$, $\mathbf{b}_{3i} = [b_i^{\mathrm{T}}\ 0]^{\mathrm{T}}$ and $\hat{\mathbf{z}} = [\,0 \quad 0 \quad 1\,]^{\mathrm{T}}$. As the actuation wrench and input twist are perpendicular zero pitch screws, the ITI for chain i is calculated according to Eqs. (3) and (5), that is

$$\mathrm{ITI}_i = \frac{{}^{\mathrm{I}}\rho_i}{{}^{\mathrm{I}}\rho_{i\max}} = \frac{{}^{\mathrm{I}}\rho_i}{a_i} = \frac{a_i \sin\beta_i}{a_i} = \sin\beta_i = |\det([\mathbf{g}_i \quad \mathbf{f}_i])| \tag{23}$$

where ${}^{\mathrm{I}}\rho_i$ is the length of the common perpendicular between the screws $\hat{\$}_{\mathrm{A},i}$ and $\hat{\$}_{\mathrm{I},i}$, ${}^{\mathrm{I}}\rho_{i\max}$ is the maximum length of ${}^{\mathrm{I}}\rho_i$ when $\hat{\$}_{\mathrm{A},i}$ is rotated about $\mathbf{c}_i$. The angle β_i is the smallest angle between the vectors $\mathbf{g}_i$ and $\mathbf{f}_i$, and a_i is the kinematic length of the upper arm link. The expression for the ITI (17) can be calculated according to

$$\mathrm{ITI}_{klm} = \min(|\det([\mathbf{g}_i \quad \mathbf{f}_i])|), \quad i = k, l, m \tag{24}$$

The ITI is zero if $\mathbf{f}_i$ and $\mathbf{g}_i$ are parallel for any of the three chains while it is one if $\mathbf{f}_i$ and $\mathbf{g}_i$ are perpendicular for all three chains.

The OTI for a nonredundant submechanism is calculated according to

$$\mathrm{OTI}_{klm} = \min(\mathrm{OTI}_k, \mathrm{OTI}_l, \mathrm{OTI}_m) \tag{25}$$

The calculation of the OTI for each of the three chains is equivalent. We here demonstrate those calculations for chain k in Fig. 3(*b*). The OTI for this chain is expressed as

$$\mathrm{OTI}_k = \left(\frac{|\hat{\$}_{\mathrm{A},k} \circ \hat{\$}_{\mathrm{O},k}|}{|\hat{\$}_{\mathrm{A},k} \circ \hat{\$}_{\mathrm{O},k}|_{\max}} \right) \tag{26}$$

where $\hat{\$}_{\mathrm{A},k}$ is the actuation wrench of chain k expressed according to Eq. (21) and the corresponding output twist $\hat{\$}_{\mathrm{O},k}$ is the platform twist when all actuators except the one of chain k are locked. The instantaneous planar motion of a rigid body can be represented as a rotation of that body, as a whole, about a fixed point in space [29]. This point of rotation is termed the instantaneous center (IC). Hence, the output twist $\hat{\$}_{\mathrm{O},k}$ is a zero pitch twist through the IC according to

$$\hat{\$}_{\mathrm{O},k} = \begin{bmatrix} \hat{\mathbf{z}} \\ \mathbf{r}_{\mathrm{IC3},k} \times \hat{\mathbf{z}} \end{bmatrix} \tag{27}$$

where the position vector of the IC is given by the planar vector $\mathbf{r}_{\mathrm{IC},k}$ or the spatial vector $\mathbf{r}_{\mathrm{IC3},k} = [\mathbf{r}_{\mathrm{IC},k}^{\mathrm{T}} \quad 0]^{\mathrm{T}}$. Utilizing that the output twist $\hat{\$}_{\mathrm{O},k}$ must be reciprocal to the actuation wrenches $\hat{\$}_{\mathrm{A},l}$ and $\hat{\$}_{\mathrm{A},m}$ provides two expressions for $\mathbf{r}_{\mathrm{IC3},k}$

$$\hat{\$}_{\mathrm{A},l} \circ \hat{\$}_{\mathrm{O},k} = \mathbf{f}_{3l} \cdot (\mathbf{r}_{\mathrm{IC3},k} \times \hat{\mathbf{z}}) + (\mathbf{d}_{3l} \times \mathbf{f}_{3l}) \cdot \hat{\mathbf{z}} = \det([\mathbf{f}_l \quad \mathbf{r}_{\mathrm{IC},k}]) - \det([\mathbf{f}_l \quad \mathbf{d}_l]) = 0 \tag{28}$$

$$\hat{\$}_{\mathrm{A},m} \circ \hat{\$}_{\mathrm{O},k} = \mathbf{f}_{3m} \cdot (\mathbf{r}_{\mathrm{IC3},k} \times \hat{\mathbf{z}}) + (\mathbf{d}_{3m} \times \mathbf{f}_{3m}) \cdot \hat{\mathbf{z}} = \det([\mathbf{f}_m \quad \mathbf{r}_{\mathrm{IC},k}]) - \det([\mathbf{f}_m \quad \mathbf{d}_m]) = 0 \tag{29}$$

Solving Eqs. (28) and (29) for the location of the IC leads to

$$\mathbf{r}_{\mathrm{IC},k} = \frac{1}{\det([\mathbf{f}_l \quad \mathbf{f}_m])} [\mathbf{f}_m \quad -\mathbf{f}_l] \begin{bmatrix} \det([\mathbf{f}_l \quad \mathbf{d}_l]) \\ \det([\mathbf{f}_m \quad \mathbf{d}_m]) \end{bmatrix} \tag{30}$$

The position $\mathbf{r}_{\mathrm{IC},k}$ is marked in Fig. 3(*b*). As expected, the IC is located at the intersection between one line specified by the position $\mathbf{d}_l$ and the vector $\mathbf{f}_l$ and another line defined by the position $\mathbf{d}_m$ and the vector $\mathbf{f}_m$. Two special cases exist when the lines are parallel, which means that the denominator in Eq. (30) is zero. If the lines are parallel but not collinear, the numerator in Eq. (30) is not zero. In this case, the IC is located at infinity, meaning a translation equals a rotation around a point in infinity. For such configurations, the output twist $\hat{\$}_{\mathrm{O},k}$ can also be expressed as a infinite pitch twist perpendicular to the actuation wrenches $\hat{\$}_{\mathrm{A},l}$ and $\hat{\$}_{\mathrm{A},m}$; however, this is not required for our purpose. The second special case occurs if the two lines are collinear, in which case also the numerator in Eq. (30) equals zero. This may be interpreted as if every point on these lines is an IC, meaning infinitesimal rotation is possible around any axis that is parallel to $\hat{\mathbf{z}}$ and intersects the collinear lines, including one axis at infinity. For such configurations, the OTI defined by Eq. (26) will always be zero. Excluding this case, we introduce the variables ${}^{\mathrm{O}}\boldsymbol{\rho}_{k\max}$ and ${}^{\mathrm{O}}\rho_{k\max}$ according to

$${}^{\mathrm{O}}\boldsymbol{\rho}_{k\max} = \mathbf{d}_k - \mathbf{r}_{\mathrm{IC},k} \tag{31}$$

$${}^{\mathrm{O}}\rho_{k\max} = ||{}^{\mathrm{O}}\boldsymbol{\rho}_{k\max}||_2 \tag{32}$$

where the distance ${}^{\mathrm{O}}\rho_{k\max}$ is marked in Fig. 3(*b*).

The OTI for chain k is calculated by expressing the output twist as a zero pitch screw through the IC and employing Eqs. (3) and (5), which leads to

$$\mathrm{OTI}_k = \frac{{}^{\mathrm{O}}\rho_k}{{}^{\mathrm{O}}\rho_{k\max}} = \frac{{}^{\mathrm{O}}\rho_{k\max} \sin\alpha_k}{{}^{\mathrm{O}}\rho_{k\max}} = \sin\alpha_k \tag{33}$$

where $\sin\alpha_k$ is the smallest angle between ${}^{\mathrm{O}}\boldsymbol{\rho}_{k\max}$ and $\mathbf{f}_k$. In the Appendix, it is shown how OTI_k may instead be expressed using only the joint positions $\mathbf{d}_k$, $\mathbf{d}_l$, $\mathbf{d}_m$ and the vectors $\mathbf{f}_k$, $\mathbf{f}_l$ and $\mathbf{f}_m$. In addition, the calculation effort required to determine the index is outlined.

The special case ${}^{\mathrm{O}}\rho_k = {}^{\mathrm{O}}\rho_{k\max} = 0$ signals a type two singularity of the mechanism. In such configurations, the OTI is zero by definition. As previously discussed, utilizing a local maximum of ${}^{\mathrm{O}}\rho_{k\max}$ to calculate OTI_k may lead to a high value of this index when ${}^{\mathrm{O}}\rho_{k\max}$ is close to zero. Hence, the index is discontinuous at ${}^{\mathrm{O}}\rho_{k\max} = 0$. Although the transmission when ${}^{\mathrm{O}}\rho_{k\max}$ is close to zero may be good in a mathematical sense, such configurations should be avoided. Due to numerical and mechanical inaccuracies, the configuration may actually be singular and even if it is not a singularity, such configurations exhibit high amplification between the actuator motion and the platform motion, leading to reduced accuracy of the mechanism. As previously mentioned, employing a global maximum of ${}^{\mathrm{O}}\rho_{k\max}$ leads to other issues and was not deemed to be a useful solution. In order to avoid division by zero, the numerical calculations required for this paper are implemented to give $\mathrm{OTI}_k = 0$ when ${}^{\mathrm{O}}\rho_{k\max}$ is below a threshold p, selected to be $1.0\,\mu$m. In order to evaluate how strongly the described issue affects the values of the fault tolerance indices, simulations were also performed for significantly larger values of p. Although effects in OTI_k were clearly seen for $p = 0.03$ m, their main effect was to reduce already low values of OTI_k further and the resulting effects on the calculated fault tolerance indices were insignificant. Increasing the value of p further, these effects became more visible.

The OTI for the studied nonredundant submechanism is calculated according to

$$\mathrm{OTI}_{klm} = \min(\mathrm{OTI}_k, \mathrm{OTI}_l, \mathrm{OTI}_m) = \min(\sin\alpha_k, \sin\alpha_l, \sin\alpha_m) \tag{34}$$

The special case of collinear actuation wrenches of two of the chains leads to a zero OTI value for the third chain and hence $\mathrm{OTI}_{klm} = 0$.

We now turn our attention to calculating the ITI, LMTI, and fault tolerance of the redundantly actuated mechanism in Fig. 2. The ITI of this redundantly actuated mechanism is calculated according to Eq. (7) as

$$\mathrm{ITI} = \min(|\det([\mathbf{g}_i \quad \mathbf{f}_i])|), \quad i = 1 \ldots 5 \tag{35}$$

while its LMTI is calculated according to Eq. (11) as

$${}^{5}\mathrm{LMTI}_{12345} = \max(\mathrm{OTI}_{\mathbf{N}_i}), \quad i = 1 \ldots 10 \tag{36}$$

where $\mathbf{N}_i$ is the i:th 3-combination of $\{1, 2, 3, 4, 5\}$ according to Eq. (10). The output fault tolerance index F_{O1} for removing one arbitrary link is calculated according to Eq. (12) as

$$F_{O1} = \min({}^4\mathrm{LMTI}_{\mathbf{E}_i}), \quad i = 1\ldots5 \tag{37}$$

where $\mathbf{E}_i$ is the i:th 4-combination of {1,2,3,4,5} according to Eq. (13). Each of the five values of ${}^4\mathrm{LMTI}_{\mathbf{E}_i}$ in Eq. (37) is the LMTI of a redundantly actuated mechanism with four actuated chains, which according to Eq. (11) can be calculated as

$${}^4\mathrm{LMTI}_{\mathbf{E}_i} = \max(\mathrm{OTI}_{\mathbf{N}_j}), \quad j = 1\ldots4 \tag{38}$$

where $\mathbf{N}_j$ is the j:th 3-combination of $\mathbf{E}_i$.

The values of $\mathrm{OTI}_{\mathbf{N}_j}$ in Eqs. (36) and (38) are the OTI for a mechanism with three remaining kinematic chains k, l, and m, which is calculated according to Eq. (34).

The input–output fault tolerance index F_{IO1} is determined by taking the minimum of F_{O1} and the ITI value of the redundant mechanism according to Eq. (14).

For the studied mechanism, the actuation wrench, input twist, and output twist are zero pitch screws. Hence, the calculated indices are immediately related to the worst-case transmission angles between the corresponding wrench and twist pairs, that is, the values of the angles α_k and β_i in Fig. 3. An acceptable range between δ and $180 - \delta$, with δ in the range 40–45 deg, has been given in Refs. [30,31]. However, this is quite conservative, particularly if used in a worst-case scenario, as for the fault tolerance indices. A value of 40 deg corresponds to a fault tolerance index of $\sin(40) = 0.64$.

For the mechanism configuration in Fig. 2(*a*), $\mathrm{ITI} = 0.6973$, ${}^5\mathrm{LMTI}_{12345} = 0.9814$ and $F_{O1} = F_{IO1} = 0.6793$. The value of ITI equals the ITI value of chain three, which is the lowest in this configuration as the elbow angle of this chain is furthest from 90 deg. The high value of ${}^5\mathrm{LMTI}_{12345}$ means that it is possible to remove two of the five chains to achieve a three chain mechanism in a near optimal configuration. As the ITI value is larger than the value of F_{O1}, the fault tolerance indices F_{O1} and F_{IO1} are equal in this configuration.

The plots in Fig. 4 show the results when analyzing the fault tolerance of the mechanism in Fig. 2 in the same central position ($x = y = 0$) for all rotation angles (ϕ). The step size in ϕ during

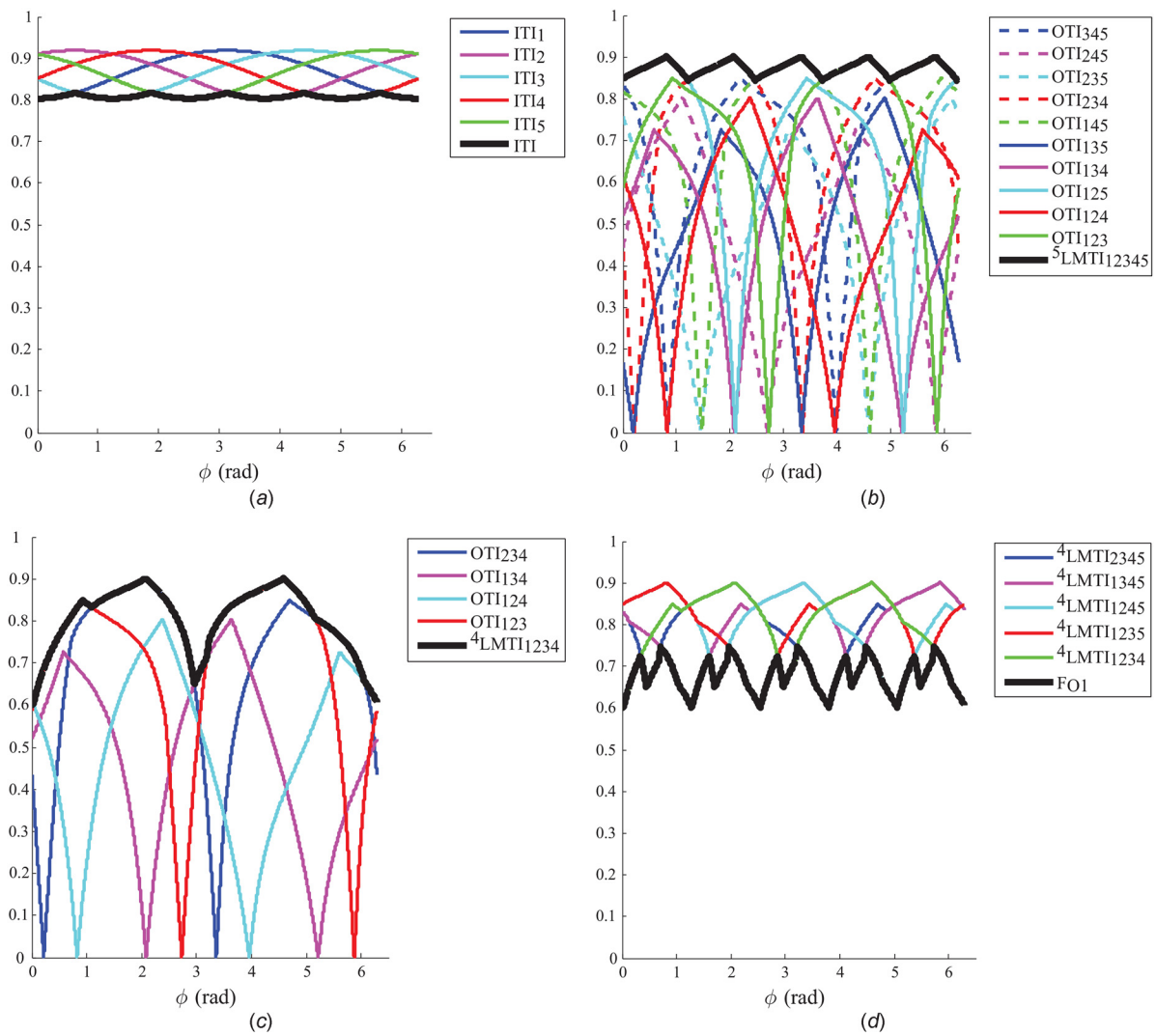

Fig. 4 Analysis of the mechanism in Fig. 2 for the same position ($x = y = 0$) and all platform angles (ϕ). (*a*) The ITI value drawn in bold is the minimum of the ITI values for each of the five chains, which are drawn using narrow lines, (*b*) The LMTI of the redundantly actuated mechanism in Fig. 2 is drawn in bold while the narrow lines show the OTI of the ten nonredundant submechanisms required to calculate the LMTI, (*c*) The LMTI of the redundantly actuated submechanism not including link 5 is drawn in bold while the narrow lines show the OTI of the four nonredundant submechanisms required to calculate the LMTI, and (*d*) The output fault tolerance index F_{O1} is drawn in bold while the narrow lines show the LMTI for the five possible redundantly actuated mechanisms that can be obtained by removing one chain from the mechanism in Fig. 2(*a*).

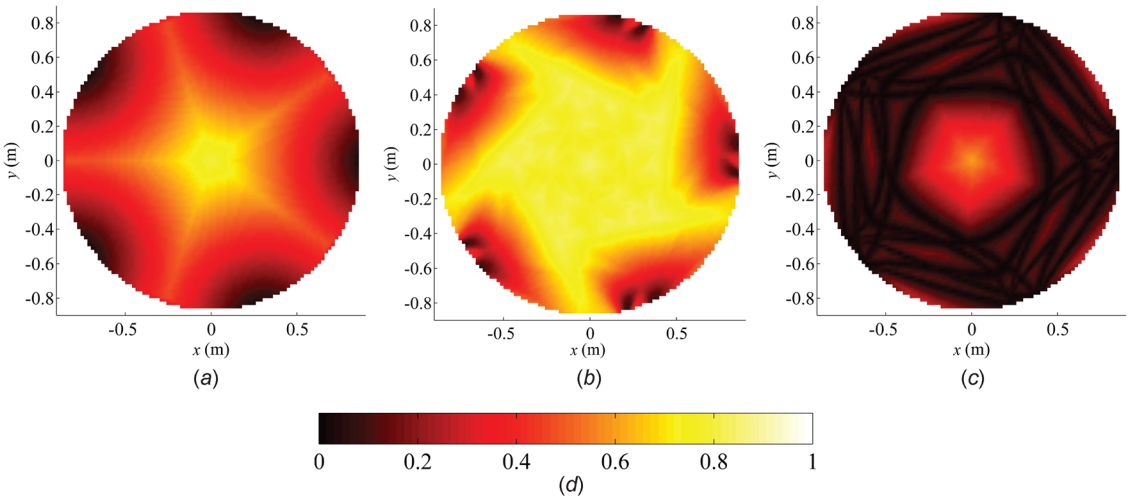

Fig. 5 The positional workspace of the mechanism in Fig. 2. Each position is marked according to the lowest value of the studied index during a 360 deg platform rotation. (*a*) The ITI value, (*b*) The $^{5}\text{LMTI}_{12345}$ value, (*c*) The output fault tolerance index F_{O1}, and (*d*) The color map used for all plots. See figure online for color.

the simulation was 0.1 deg and no significant difference was seen using a larger step size of 1 deg.

Figure 4(*a*) shows the ITI value for the studied mechanism. This value is the minimum of the ITI of the five kinematic chains. The high value in these central configurations indicates a large distance to any type one singularity.

Figure 4(*b*) shows $^{5}\text{LMTI}_{12345}$ for the studied mechanism, which is the LMTI of the redundantly actuated mechanism in Fig. 2(*a*). According to Eq. (36), this LMTI value is the maximum of the OTI of ten possible nonredundant submechanisms. Each OTI distribution exhibits two zeros during a 360 deg rotation, corresponding to output transmission singularities, also known as parallel singularities or type two singularities.

Figure 4(*c*) shows $^{4}\text{LMTI}_{1234}$, which is the LMTI for a mechanism where chain five has been removed. As seen in Eq. (38), the LMTI value is the maximum of the OTI of four possible nonredundant submechanisms. Comparing the bold lines in Fig. 4(*b*) and (*c*) five highlights the benefit of including chain five in the mechanism.

Figure 4(*d*) shows the index F_{O1}. In this central workspace location, the index is above 0.6 for all platform orientations. The index is determined from the minimum of five LMTI values. Because the ITI value is larger than the value of F_{O1} in Fig. 4(*d*), the fault tolerance indices F_{O1} and F_{IO1} are equal in these configurations. A minimum value of 0.6 means that for the worst-case fault in the worst investigated configuration, it is possible to use three of the four remaining chains to form a nonredundant submechanism where the three transmission angles α_i are between 37 and 143 deg ($\sin(37) = \sin(143) = 0.6$). It is reasonable to state that in this central location, the mechanism is fault tolerant for losing one arbitrary link.

Figure 5 shows an evaluation of the mechanism in a circular workspace section with the center in the origin of the coordinate system **F** in Fig. 2(*a*). The circle radius was selected to avoid potential collisions between the manipulated platform and the base joints and between the platform and the upper arm links. The step size in x and y was 0.02 m. For each studied position, platform angles between 0 and 360 deg were evaluated, where the angular step size was 1 deg. The color in each position was selected based on the lowest value of each studied index during a full platform rotation, according to the color map in Fig. 5(*d*) (see figures online for color).

Figure 5(*a*) shows the ITI distribution. Within a circle of radius 0.5 m, the ITI value is above 0.5. Referring to Fig. 3(*a*), this corresponds to $\beta_i = 30$ deg or $\beta_i = 150$ deg for the worst performing chain in the worst configuration.

Figure 5(*b*) illustrates $^{5}\text{LMTI}_{12345}$. Due to the double actuation redundancy, the majority of the positional workspace permits infinite rotation of the tool platform with a large LMTI value.

Figure 5(*c*) shows the value of the F_{O1} index. Within a circle of radius 0.2 m, the F_{O1} value is above 0.4. Hence, within this workspace area, for the worst-case fault in the worst investigated configuration, it is possible to use three of the four remaining chains to form a nonredundant submechanism where the three transmission angles α_i are between 24 and 156 deg. Although this is not within the 40–140 deg range recommended in Refs. [30,31], it is still sufficient for the mechanism to perform many tasks. Although the exact requirement on the minimum transmission angle is application dependent, within this area the mechanism can be considered fault tolerant for an arbitrary linkage disappearing. Outside the central region, there is a complex web of locations with very low values of the index. This area of the workspace cannot be considered fault tolerant.

Due to the relatively high value of ITI in the studied workspace range, the plot of F_{IO1} is almost identical to F_{O1} illustrated in Fig. 5(*c*) and therefore not included here. By moving the base joint position $\mathbf{b}_i$ in Fig. 2(*a*) toward the center, the elbow angles at $\mathbf{c}_i$ become smaller, leading to smaller ITI values and a larger differentiation between the two indices.

5 Conclusion and Future Work

This paper introduced two novel fault tolerance indices for redundantly actuated parallel mechanisms. The proposed indices are based on the normalized reciprocal product between a wrench and a twist. The faults considered are free-swinging joint failures, that is, failures that can be interpreted as one or more actuated joints becoming passive. However, for a large range of mechanisms, the proposed indices are also applicable to failures corresponding to the disappearance of a kinematic chain, for example, the breakage of a link. The main advantage of the proposed indices is their applicability to redundantly actuated parallel mechanisms with arbitrary DOFs. The feasibility of the proposed indices was demonstrated by their application to a 3-DOF planar mechanism of this type.

An interesting avenue for future work is to employ the proposed indices to find optimal architectures of fault tolerant mechanisms of various mobility. For example, determining the architecture that maximizes the fault tolerant workspace of the mechanism in Sec. 4, that is, the architecture that maximizes the central region in Fig. 5. Architectures designed for optimal fault tolerance are

likely to be significantly different compared to architectures designed for other purposes.

Appendix: Calculation Effort

In this appendix, we discuss the calculation effort of determining the OTI. The value of OTI_k, given by Eq. (33), may be expressed as

$$\mathrm{OTI}_k = \sin\alpha_k = \left|\det\left(\begin{bmatrix} {}^{\mathrm{O}}\boldsymbol{\rho}_{k\max} \\ {}^{\mathrm{O}}\rho_{k\max} \end{bmatrix} \quad \mathbf{f}_k \right)\right| \tag{A1}$$

Utilizing Eqs. (30)–(32), Eq. (A1) may be rewritten according to

$$\mathrm{OTI}_k = \frac{\mathrm{abs}(|\mathbf{f}_k\ \mathbf{d}_k||\mathbf{f}_l\ \mathbf{f}_m| + |\mathbf{f}_l\ \mathbf{d}_l||\mathbf{f}_m\ \mathbf{f}_k| + |\mathbf{f}_m\ \mathbf{d}_m||\mathbf{f}_k\ \mathbf{f}_l|)}{\mathrm{abs}(|\mathbf{f}_l\ \mathbf{f}_m|)^{\mathrm{O}}\rho_{k\max}} \tag{A2}$$

In order to achieve a clear and compact formulation of Eq. (A2), we have used the notation $|\mathbf{x}\ \mathbf{y}|$ instead of $\det([\mathbf{x}\ \mathbf{y}])$ and $\mathrm{abs}(x)$ instead of $|x|$. The numerator in Eq. (A2) is equal for all permutations of k, l, and m, meaning it only has to be calculated once for each nonredundant manipulator. Interestingly, this also means that the instantaneous work described by $\hat{\$}_{\mathrm{A},k} \circ \hat{\$}_{\mathrm{O},k}$ for one chain k is related to the instantaneous work of chains l and m according to

$$\begin{aligned}\mathrm{abs}((\hat{\$}_{\mathrm{A},k} \circ \hat{\$}_{\mathrm{O},k})|\mathbf{f}_l\ \mathbf{f}_m|) &= \mathrm{abs}((\hat{\$}_{\mathrm{A},l} \circ \hat{\$}_{\mathrm{O},l})|\mathbf{f}_k\ \mathbf{f}_m|) \\ &= \mathrm{abs}((\hat{\$}_{\mathrm{A},m} \circ \hat{\$}_{\mathrm{O},m})|\mathbf{f}_k\ \mathbf{f}_l|)\end{aligned} \tag{A3}$$

Equation (A3) is also valid when two links are parallel, as long as they are not collinear. A value of $|\mathbf{f}_l\ \mathbf{f}_m| = 0$ means that the IC is at infinity and therefore an infinite value of $\hat{\$}_{\mathrm{A},k} \circ \hat{\$}_{\mathrm{O},k}$; however, employing Eq. (30) leads to a finite product between $|\mathbf{f}_l\ \mathbf{f}_m|$ and $(\hat{\$}_{\mathrm{A},k} \circ \hat{\$}_{\mathrm{O},k})$.

By employing Eqs. (30)–(32), Eq. (A2) may be expressed according to

$$\mathrm{OTI}_k = \frac{\mathrm{abs}(|\mathbf{f}_k\ \mathbf{d}_k||\mathbf{f}_l\ \mathbf{f}_m| + |\mathbf{f}_l\ \mathbf{d}_l||\mathbf{f}_m\ \mathbf{f}_k| + |\mathbf{f}_m\ \mathbf{d}_m||\mathbf{f}_k\ \mathbf{f}_l|)}{\sqrt{|\mathbf{f}_l\ \mathbf{f}_m|^2||\mathbf{d}_k||_2^2 - 2|\mathbf{f}_l\ \mathbf{f}_m|\mathbf{d}_k^{\mathrm{T}}[\mathbf{f}_m - \mathbf{f}_l]\begin{bmatrix}|\mathbf{f}_l\ \mathbf{d}_l| \\ |\mathbf{f}_m\ \mathbf{d}_m|\end{bmatrix} + \left|\left|[\mathbf{f}_m - \mathbf{f}_l]\begin{bmatrix}|\mathbf{f}_l\ \mathbf{d}_l| \\ |\mathbf{f}_m\ \mathbf{d}_m|\end{bmatrix}\right|\right|_2^2}} \tag{A4}$$

This expression is valid also if $\mathbf{f}_l$ and $\mathbf{f}_m$ are parallel ($|\mathbf{f}_l\ \ \mathbf{f}_m| = 0$). In this case, the first term in the numerator and the first two terms in the square-root expression disappear and Eq. (A4) simplifies to

$$\mathrm{OTI}_k = \frac{\mathrm{abs}(|\mathbf{f}_l\ \mathbf{d}_l||\mathbf{f}_m\ \mathbf{f}_k| + |\mathbf{f}_m\ \mathbf{d}_m||\mathbf{f}_k\ \mathbf{f}_l|)}{\left|\left|[\mathbf{f}_m - \mathbf{f}_l]\begin{bmatrix}|\mathbf{f}_l\ \mathbf{d}_l| \\ |\mathbf{f}_m\ \mathbf{d}_m|\end{bmatrix}\right|\right|_2} \tag{A5}$$

Inserting $\mathbf{f}_m = \mathbf{f}_l$ in Eq. (A5) and simplifying leads to

$$\mathrm{OTI}_k = \mathrm{abs}(|\mathbf{f}_l\ \mathbf{f}_k|) \tag{A6}$$

which is identical to the expression for OTI_k achieved if the output twist $\hat{\$}_{\mathrm{O},k}$ is expressed as an infinite pitch twist instead of a zero pitch twist at infinity.

According to Eqs. (37) and (38), 20 values of OTI for nonredundant submanipulators must be determined; however, not all of them are unique. As the OTI for a nonredundant manipulator depends on the configuration of all three chains, OTI_{klm} must only be determined for $\binom{5}{3} = 10$ different nonredundant manipulators. The value of OTI_{klm} is in turn calculated by the minimum of three chains, employing Eqs. (34) and (A4). The numerator of Eq. (A4) is identical for all three chains, while the denominator is chain dependent. Hence, in each configuration of the manipulator in Fig. 2(*a*), the numerator of Eq. (A4) must be calculated ten times and the denominator 30 times. As can be seen from Eqs. (35) and (14), the additional calculations required to determine $\mathrm{F}_{\mathrm{IO1}}$ are comparatively minor.

References

[1] Maciejewski, A. A., 1990, "Fault Tolerant Properties of Kinematically Redundant Manipulator," IEEE International Conference on Robotics and Automation (ICRA'90), pp. 638–642.

[2] Roberts, R. G., and Maciejewski, A. A., 1996, "A Local Measure of Fault Tolerance for Kinematically Redundant Manipulators," IEEE Trans. Rob. Autom., **12**(4), pp. 543–552.

[3] Lewis, C. L., and Maciejewski, A. A., 1997, "Fault Tolerant Operation of Kinematically Redundant Manipulators for Locked Joint Failures," IEEE Trans. Rob. Autom., **13**(4), pp. 622–629.

[4] English, J. D., and Maciejewski, A. A., 1998, "Fault Tolerance for Kinematically Redundant Manipulators: Anticipating Free-Swinging Joint Failures," IEEE Trans. Rob. Autom., **14**(4), pp. 566–575.

[5] Matone, R., and Roth, B., 1999, "In-Parallel Manipulators: A Framework on How to Model Actuation Schemes and a Study of Their Effects on Singular Postures," ASME J. Mech. Des., **121**(1), pp. 2–8.

[6] English, J. D., and Maciejewski, A. A., 2001, "Failure Tolerance Through Active Braking: A Kinematic Approach," Int. J. Rob. Res., **20**(4), pp. 287–299.

[7] Zhao, J., Zhang, K., and Yao, X., 2006, "Study on Fault Tolerant Workspace and Fault Tolerant Planning Algorithm Based on Optimal Initial Position for Two Spatial Coordinating Manipulators," Mech. Mach. Theory, **41**(5), pp. 584–595.

[8] Tinós, R., Terra, M. H., and Bergerman, M., 2007, "A Fault Tolerance Framework for Cooperative Robotic Manipulator," Control Eng. Pract., **15**(5), pp. 615–625.

[9] O'Brien, J. F., and Wen, J. T., 1999, "Redundant Actuation for Improving Kinematic Manipulability," IEEE International Conference on Robotics and Automation (ICRA'99), pp. 1520–1525.

[10] Notash, L., and Huang, L., 2003, "On the Design of Fault Tolerant Parallel Manipulators," Mech. Mach. Theory, **38**(1), pp. 85–101.

[11] Yi, Y., McInroy, J. E., and Chen, Y., 2006, "Fault Tolerance of Parallel Manipulators Using Task Space and Kinematic Redundancy," IEEE Trans. Rob., **22**(5), pp. 1017–1021.

[12] Marlow, K., Isaksson, M., and Nahavandi, S., 2016, "Motion/Force Transmission Analysis of Planar Parallel Mechanisms With Closed-Loop Subchains," ASME J. Mech. Rob., **8**(4), p. 041019.

[13] Ball, R. S., 1900, *A Treatise on the Theory of Screws*, Cambridge University Press, New York.

[14] Sutherland, G., and Roth, B., 1973, "A Transmission Index for Spatial Mechanisms," J. Eng. Ind., **95**(2), pp. 589–597.

[15] Tsai, M. J., and Lee, H. W., 1994, "The Transmissivity and Manipulability of Spatial Mechanisms," ASME J. Mech. Des., **116**(1), pp. 137–143.

[16] Chen, C., and Angeles, J., 2007, "Generalized Transmission Index and Transmission Quality for Spatial Linkages," Mech. Mach. Theory, **42**(9), pp. 1225–1237.

[17] Wang, J., Wu, C., and Liu, X.-J., 2010, "Performance Evaluation of Parallel Manipulators: Motion/Force Transmissibility and Its Index," Mech. Mach. Theory, **45**(10), pp. 1462–1476.

[18] Xie, F., Liu, X.-J., and Li, J., 2014, "Performance Indices for Parallel Robots Considering Motion/Force Transmissibility," *Intelligent Robotics and Applications* (Lecture Notes in Computer Science), Vol. 8917, Springer Berlin, pp. 35–43.

[19] Liu, X.-J., Chen, X., and Nahon, M., 2014, "Motion/Force Constrainability Analysis of Lower-Mobility Parallel Manipulators," ASME J. Mech. Rob., **6**(3), p. 031006.

[20] Liu, H., Wang, M., Huang, T., Chetwynd, D. G., and Kecskeméthy, A., 2015, "A Dual Space Approach For Force/Motion Transmissibility Analysis of Lower Mobility Parallel Manipulators," ASME J. Mech. Rob., **7**(3), p. 034504.

[21] Marlow, K., Isaksson, M., Dai, J. S., and Nahavandi, S., 2016, "Motion/Force Transmission Analysis of Parallel Mechanisms With Planar Closed-Loop Sub-Chains," ASME J. Mech. Des., **138**(6), p. 062302.

[22] Gosselin, C., and Angeles, J., 1990, "Singularity Analysis of Closed-Loop Kinematic Chains," IEEE Trans. Rob. Autom., **6**(3), pp. 281–290.
[23] Zlatanov, D., Bonev, I. A., and Gosselin, C. M., 2002, "Constraint Singularities of Parallel Mechanisms," IEEE International Conference on Robotics and Automation (ICRA'01), pp. 496–502.
[24] Liu, X.-J., Wu, C., and Wang, J., 2012, "A New Approach for Singularity Analysis and Closeness Measurement to Singularities of Parallel Manipulators," ASME J. Mech. Rob., **4**(4), p. 041001.
[25] Xie, F., Liu, X.-J., and Wang, J., 2011, "Performance Evaluation of Redundant Parallel Manipulators Assimilating Motion/Force Transmissibility," Int. J. Adv. Rob. Syst., **8**(5), pp. 113–124.
[26] Liu, G. F., Wu, Y. L., Wu, X. Z., Kuen, Y. Y., and Li, Z. X., 2001, "Analysis and Control of Redundant Parallel Manipulators," IEEE International Conference on Robotics and Automation (ICRA'01), pp. 3748–3754.
[27] Kurtz, R., and Hayward, V., 1992, "Multiple-Goal Kinematic Optimization of a Parallel Spherical Mechanism With Actuator Redundancy," IEEE Trans. Rob. Autom., **8**(5), pp. 644–651.
[28] Nokleby, S. B., Fisher, R., Podhorodeski, R. P., and Firmani, F., 2005, "Force Capabilities of Redundantly-Actuated Parallel Manipulators," Mech. Mach. Theory, **40**(5), pp. 578–599.
[29] Phakatkar, H. G., 1987, *A Text Book of Theory of Machines and Mechanisms–I*, 4th ed., Nirali Prakashan, Pune, India.
[30] Wu, C., Liu, X.-J., Wang, L., and Wang, J., 2010, "Optimal Design of Spherical 5R Parallel Manipulators Considering the Motion/Force Transmissibility," ASME J. Mech. Des., **132**(3), p. 031002.
[31] Wang, J., Liu, X.-J., and Wu, C., 2009, "Optimal Design of a New Spatial 3-DOF Parallel Robot With Respect to a Frame-Free Index," Sci. China, Ser. E: Technol. Sci., **52**(4), pp. 986–999.